actuators

MDPI

Article

Bridging Regimes: A State-Dependent Blending Methodology for Parsimonious and Robust Heavy Vehicle Dynamics Modeling

Ozgur Unsal [1,*] and Hakan Yavuz [2]

[1] TEMSA, 01110 Adana, Türkiye
[2] Cukurova University, Engineering Faculty, Mechanical Engineering Department, 01330 Adana, Türkiye; hyavuz@cu.edu.tr
* Correspondence: ozgur.unsal@temsa.com

Abstract

Data-driven gray-box models for vehicle control often fail to generalize across distinct physical regimes. This study tackles the critical, yet often-overlooked, challenge of robustly blending model parameters between these regimes. The vehicle's "expert poles" are defined using physically distinct maneuvers (steady state vs. transient). A three-way benchmark is used to prove that the blending method is more critical than the concept itself. Three architectures are compared: (1) a baseline single-parameter "Static Model", (2) a common literature "Heuristic Model" that blends using lateral acceleration (a_y), and (3) the proposed "Dynamic Model" using a systematically optimized "Angle-Only" architecture. The findings demonstrate significant differences: The common-sense "Heuristic Model" exhibits severe degradation in stability metrics, lowering overall a_y accuracy by 23.7% and r (yaw rate) accuracy by 110.2% compared to the baseline. In contrast, the "Angle-Only" model is the only architecture that successfully improves the primary a_y objective (by 17.7%). The Dynamic Model's 35.0% r-metric degradation is demonstrated to be the minimal, quantified engineering trade-off required for achieving robust adaptation—a task completely failed by the Heuristic Model. This study provides a validated, data-driven path for developing control-oriented models, proving that a simple, systematically optimized input is methodologically superior to the state-dependent heuristic.

Keywords: vehicle dynamics; system identification; gray-box modeling; state-dependent blending; principle of parsimony; model generalization

1. Introduction

Accurate and physically robust dynamic models of heavy vehicles (HVs) are essential for developing advanced driver-assistance systems (ADASs) and for the growing reliance on virtual validation in the transport industry [1,2]. However, creating such models from limited experimental data is far from trivial. The process is constrained by what may be termed a modeling trilemma—the competing demands of predictive accuracy, computational efficiency, and physical plausibility [2]. This challenge is amplified by the scarcity of experimental data, as limit-handling tests are costly, difficult to replicate, and often unreproducible in identical conditions. As famously stated by George Box, "All models are wrong, but some are useful." This maxim is particularly relevant to heavy-vehicle dynamics, where the goal is not perfect replication but a practically useful, robust, and physically credible model derived from sparse data [3,4].

Check for updates

Academic Editor: Xiaozheng Jin

Received: 17 November 2025
Revised: 8 December 2025
Accepted: 17 December 2025
Published: 19 December 2025

Copyright: © 2025 by the authors. Licensee MDPI, Basel, Switzerland. This article is an open access article distributed under the terms and conditions of the Creative Commons Attribution (CC BY) license.

Traditional high-fidelity "white-box" models, while physically detailed, tend to violate efficiency and identifiability constraints, making them impractical for real-world estimation and control applications. In contrast, low-order "gray-box" models often sacrifice too much accuracy in pursuit of parsimony. This tension motivates the present study to develop a methodology that strategically balances these competing objectives, achieving the greatest possible adaptability and physical plausibility under data-sparse conditions [5].

A common starting point in this domain is the development of parsimonious gray-box models that combine simplified physical structure with empirically identified parameters. A foundational version of such a model, referred to here as the Static Model, adopted a single, globally optimized parameter set to represent the vehicle's dynamic behavior. Yet, detailed analysis revealed a critical structural limitation: a single parameterization, no matter how well tuned, cannot capture the complex, state-dependent behavior of a vehicle across its full operational envelope [6]. The effective stiffness, damping, and handling characteristics of heavy vehicles vary markedly between quasi-steady-state turning and highly transient maneuvers [7–9]. Consequently, the Static Model's limitation lies not in its simplicity, but in the flawed assumption that a single set of parameters can remain universally valid across dynamic regimes.

The state of the art presents a wide spectrum of vehicle modeling philosophies. At one extreme, high-fidelity multi-body simulation (MBS) models capture detailed physical dynamics but suffer from overparameterization and limited identifiability when faced with sparse data [10–13]. Even when successfully tuned, these models often exhibit narrow validity: a configuration calibrated for an ISO lane-change maneuver may not generalize to quasi-steady-state cornering without extensive reparameterization. At the other extreme, purely data-driven "black-box" models, such as deep neural networks, excel in fitting complex nonlinearities but risk producing physically implausible behavior, especially outside the training domain [14–17].

Between these extremes lies the pragmatic "gray-box" philosophy, which this study embraces. Related efforts in gain scheduling (GS) and fuzzy logic control (FLC) have demonstrated that model blending can significantly enhance adaptability [18,19]. For instance, it was demonstrated by Saleem et al. [20] that hierarchical fuzzy-adaptive mechanisms can effectively suppress structural vibrations by dynamically tuning control parameters, a concept analogous to the regime-dependent parameter blending proposed in this study. However, the effectiveness of these methods hinges on the choice of the scheduling variable—the signal governing how local models are interpolated. Many existing approaches rely on heuristic variables (e.g., speed, steering angle, or lateral acceleration), resulting in models that are either sensitive to noise or dependent on unavailable signals. Furthermore, much of the existing HV literature validates model performance against high-fidelity simulations (e.g., MBM to RTM) rather than real-world experimental data, due to the prohibitive cost and difficulty of full-scale testing [21]. This study addresses this gap by using real vehicle data from distinct maneuvers as the definitive ground truth for assessing model plausibility, stability, and generalization.

While the primary focus of vehicle dynamics modeling has traditionally been on paved, structured environments, recent research highlights the critical need for robust models capable of handling unstructured terrain. As demonstrated by Nowakowski and Kosiuczenko [22] in their analysis of UGV deployment in unstructured terrain and by Dantas and Faria [23] regarding the influence of unpaved-road conditions on heavy-vehicle dynamics, real-world operational envelopes are fraught with environmental disturbances that challenge static parameterizations. In such regimes, the effective stiffness and damping of the system can vary drastically, necessitating a model structure that is inherently adaptive.

In the broader control literature, Linear Parameter-Varying (LPV) and State-Dependent Riccati Equation (SDRE) methods have set the benchmark for such adaptability. H∞/LPV approaches were demonstrated by Vu et al. [24] for active anti-roll bars, while the SDRE framework was utilized by Tjønnås and Johansen [25] for control allocation. However, these frameworks often rely on the assumption that a robust scheduling variable is available a priori. As noted by Németh et al. [26], the "selection of the scheduling variable" itself is a critical stability bottleneck in data-sparse conditions. Furthermore, as shown by Zatout et al. [27], the optimization of heuristic structures is essential to ensure stability across diverse operating conditions.

This specific research gap is addressed in this study, the primary objective of which is to develop a methodologically robust blending architecture that enables parsimonious gray-box models to generalize across distinct physical regimes without relying on complex black-box structures or noise-sensitive heuristic variables.

To clarify the distinctions among existing methodologies, Table 1 summarizes representative studies that span the full modeling spectrum—from high-fidelity physical formulations to probabilistic and hybrid data-driven approaches. Each entry highlights the study's core philosophy, architectural complexity, adaptation strategy, and contribution relative to the present work. As shown, high-fidelity multi-body and white-box models [11,12] provide detailed physics but suffer from parameter unidentifiability when data are limited. Deep-learning-based hybrids enhance nonlinear prediction but often compromise transparency and physical interpretability [28,29]. Probabilistic inference methods introduce robustness through uncertainty quantification but at a substantial computational cost. Classical gain-scheduling and FL frameworks [18] achieve adaptability but rely on heuristic or single-variable blending strategies. In contrast, the proposed study adopts a parsimony-first, methodologically robust approach that blends the interpretability of low-order physical models with the adaptability of state-dependent calibration. The comparison demonstrates that a carefully designed blending heuristic, grounded in physically distinct regimes and optimized for robustness, can deliver generalization and realism comparable to more complex alternatives, without sacrificing computational efficiency [30–32].

Table 1. Comparative overview of vehicle dynamics modeling approaches.

Study	Core Philosophy	Model Architecture and Complexity	Adaptation/Estimation Method	Key Contribution (Relative to Proposed Study)
[11]	High-Fidelity Physical (MBM to RTM)	Four Single-Track Models of increasing complexity, derived from a Multi-Body Model.	Optimization-based estimation from MBM data.	Demonstrates model simplification from a high-fidelity source, contrasting the parsimony-first principle.
[28]	Deep Learning Hybrid	3-DOF Physical Model + Transformer (DyTR) neural network.	Gradient-based training for the neural network.	Shows the power of using an NN to correct a physical model's errors; contrasts the low-dimensional, heuristic approach.
[29]	Deep Learning Hybrid (PINN)	Physics-Constrained Neural Network (PCNN) with a "Physics Guard" layer.	Gradient-based training with physics embedded in the loss function.	Integrates physics directly into the NN architecture, differing from the use of physics as optimization-level constraints.

Table 1. *Cont.*

Study	Core Philosophy	Model Architecture and Complexity	Adaptation/Estimation Method	Key Contribution (Relative to Proposed Study)
[32]	Probabilistic Inference	Bicycle model with nonlinear tire and CoG parameters.	Simulation-Based Inference (SBI) to estimate posterior probability.	Provides a full picture of parameter uncertainty, contrasting the deterministic optimization for convergence robustness.
[14]	Gain Scheduling	Linear Quadratic Regulator (LQR) controllers for different velocities.	Interpolation between pre-designed LQR controllers based on vehicle velocity.	A classic gain-scheduling approach using a single scheduling variable (velocity), whereas the proposed method uses multiple inputs.
[17]	Formal Fuzzy Logic	Takagi–Sugeno fuzzy model composed of local linear systems.	State feedback for each local linear system.	Represents a formal FLC approach, which is more complex than the computationally efficient "fuzzy-like" heuristic.
[18]	State and Parameter Estimation	Vehicle dynamic models with uncertain parameters (e.g., cornering stiffness).	Kinematic estimators combining GPS and inertial sensors.	Focuses on simultaneous state and parameter estimation, whereas the proposed approach uses offline calibration for expert models.
[31]	Bayesian Inference	Vehicle lateral dynamics model.	Bayesian method (ABC-SMC) on spline-smoothed data.	A modern approach for robust parameter estimation from noisy data, complementing the deterministic optimization focus.
Proposed Study	Parsimony-Focused, Methodologically Robust	Behavioral Lateral Model + 2-DOF Physical Roll Model (5 parameters).	Dual-regime calibration followed by a state-dependent "fuzzy-like" blending heuristic.	Proves that a dynamic blend of simple models, governed by a computationally efficient heuristic, can achieve superior generalization and physical realism.

The present study thus documents the evolution of the Static Model into an adaptive Dynamic Model through a two-stage methodology. The contribution of this study lies not in the concept of blending itself but in the development of a provably robust methodology for applying blending to sparse heavy-vehicle data. To evaluate this systematically, a Heuristic Model is also introduced as a benchmark, using identical expert parameter sets but replacing the optimized "Angle-Only" logic with a conventional lateral-acceleration-based blending rule. This direct comparison establishes whether the proposed architecture genuinely provides superior performance.

Accordingly, the main contributions of this study are threefold:

- A Regime-Targeted Calibration Methodology: The methodology demonstrates that expert models must be calibrated against physically distinct maneuvers (constant

radius for steady state and increasing steer for transient) to define the valid poles of the vehicle's state space, rejecting the assumption of a single globally valid parameter set.

- A Systematic Optimization for Blending Architecture: The architecture provides a formal process for selecting the blending variable. It is shown quantitatively that a simpler Angle-Only architecture is more robust, less noise-sensitive, and more effective than multi-input or derivative-based heuristics.
- A Quantified Plausibility–Fidelity Trade-Off: We demonstrate, through detailed results (Section 3), that prioritizing physical stability and lateral-acceleration fidelity over yaw-rate fidelity yields a model that is both stable and practically applicable—a rational engineering trade-off emphasizing realism over overfitting.

The remainder of this manuscript is organized as follows. Section 2 details the material and methods, beginning with the foundational gray-box vehicle model, including the lateral and roll dynamics subsystems, and then outlining the computational pipeline used for regime-targeted calibration based on constant-radius and increasing-steer maneuvers. This section concludes with the formulation of the optimization-driven blending architecture. Section 3 presents the results, covering the optimization of the blending structure, dual-regime calibration outcomes with their physical interpretation, and an evaluation of the model's generalization, interpolation, and robustness characteristics. Furthermore, Section 3 provides detailed analyses on performance across all dynamic regimes, limit-handling capabilities, stability, and physical plausibility under extreme conditions, as well as Monte-Carlo-based uncertainty assessments. Section 4 provides a broader discussion of the findings, emphasizing the role of blending in achieving physical realism, reframing the lateral-acceleration trade-off, and outlining limitations and directions for future research. Finally, Section 5 summarizes the key conclusions of the study.

2. Materials and Methods

This section describes the modeling framework and calibration methodology that transform the foundational static model into the adaptive, state-dependent "Dynamic Model." The process comprises three key stages:

(1) Formulation of a parsimonious gray-box vehicle model;
(2) Regime-targeted parameter calibration;
(3) Optimization-based state-dependent blending.

2.1. Foundational Gray-Box Vehicle Model

The core of the modeling framework is a five-parameter gray-box architecture that decouples lateral and roll dynamics to achieve computational efficiency while retaining physical interpretability. The model's structure is physically inspired, yet its coefficients are treated as effective parameters identified from experimental data, representing aggregated nonlinear effects such as tire saturation and suspension compliance.

(a) **Lateral Dynamics Subsystem**

The lateral dynamics are modeled using a quasi-static formulation that relates the steering input to lateral acceleration a_y and yaw rate r. The road wheel angle δ is derived from the steering wheel input δ_{sw} and the steering ratio i_s:

$$\delta = \frac{\delta_{sw}}{i_s} \tag{1}$$

A linear approximation of lateral acceleration is then computed using the classical bicycle model:

$$a_{y,\text{lin}} = \frac{u^2}{L} \tan(\delta) \tag{2}$$

where u is the longitudinal velocity, and L is the vehicle wheelbase [21].

To represent tire force saturation, a hyperbolic tangent formulation is applied, and it is governed by two behavioral parameters: the peak lateral force factor $F_{peak,lat}$ and the lateral force slope factor $F_{slope,lat}$:

$$a_y = F_{peak,lat} \tanh\left(\frac{a_{y,lin}}{F_{slope,lat}}\right) \tag{3}$$

This relationship compresses the linear growth of lateral acceleration at higher steering inputs, providing a smooth and realistic transition into the nonlinear regime.

The yaw rate r is subsequently derived as follows:

$$r = \frac{a_y}{u} \tag{4}$$

Equations (1)–(4) collectively form the behavioral lateral dynamics submodel, which captures essential steady-state and transient responses while remaining computationally minimal.

(b) **Roll Dynamics Subsystem**

The roll motion of the vehicle is represented by a second-order mass–spring–damper system, where the roll angle is ϕ, the roll rate is $\dot{\phi}$, and the roll acceleration is $\ddot{\phi}$. The governing equation of motion is as follows:

$$I_\phi \ddot{\phi} + C_\phi \dot{\phi} + K_\phi \phi = G_{roll} a_y + \phi_{road,avg} \tag{5}$$

where the variables are defined as follows:

- I_ϕ is the effective roll inertia;
- C_ϕ and K_ϕ represent roll damping and stiffness, respectively;
- G_{roll} is the roll gain coefficient;
- $\phi_{road,avg}$ is the averaged roll excitation due to the road profile.

For compactness, this can be rewritten as follows:

$$\ddot{\phi} + 2\zeta_{roll}\omega_{n,roll}\dot{\phi} + \omega_{n,roll}^2 \phi = \frac{G_{roll} a_y}{I_\phi} + \frac{\phi_{road,avg}}{I_\phi} \tag{6}$$

where $\omega_{n,roll}$ is the roll natural frequency, and ζ_{roll} is the roll damping ratio.

The full model, therefore, consists of five key tunable parameters: $\{F_{peak,lat}, F_{slope,lat}, G_{roll}, \omega_{n,roll}, \zeta_{roll}\}$.

This parsimonious formulation captures the essential lateral–roll coupling dynamics while ensuring parameter identifiability and low computational cost.

2.2. Computational Pipeline and Regime-Targeted Calibration

Following the identification of the expert parameter sets ($PARAMS_{CR}$ and $PARAMS_{IS}$) using the hybrid GA–Pattern Search method described above, a secondary optimization stage is conducted to determine the optimal blending strategy.

Data Processing Pipeline:

To ensure reproducibility, a standardized pipeline is implemented in MATLAB (Matlab 2024a). Raw experimental data (GPS, IMU, and displacement transducers) underwent the following steps:

➢ Smoothing: A smoothing spline algorithm (smoothingspline, $p \approx 0.99$) is applied to mitigate sensor quantization noise while preserving dynamic peaks.

- ➢ Analytical Differentiation: Kinematic derivatives (e.g., steering rate) are calculated analytically from the fitted spline objects to prevent noise amplification associated with numerical finite differences.
- ➢ Segmentation: Maneuvers are temporally aligned based on a steering threshold of 0.17 rad (10 degrees).

Two-Stage Optimization Strategy:

The model parameters are identified using a two-stage process to ensure physical plausibility:

- ➢ Stage 1 (Parameter Calibration): The "Expert Poles" ($PARAMS_{CR}$ and $PARAMS_{IS}$) are identified using a hybrid optimization method. A Genetic Algorithm (GA) (Pop: 60; Gen: 100) is used to perform the global search to avoid local minima, followed by a Pattern Search algorithm for local refinement. Lateral acceleration (w_{a_y}= 1.0), yaw rate (w_r = 1.75), and suspension displacement (w_{sus} = 2.0) are weighted within the cost function, with heavy penalties for physically invalid states (e.g., wheel lift).
- ➢ Stage 2 (Blending Architecture): The scheduling variable is selected via secondary optimization, minimizing the regime identification error (RMSE) using the SQP algorithm, which identified the steering angle as the sole robust predictor (see Table 2).

Table 2. Blending architecture optimization results.

Input Variable	Optimized Weight (w)	Normalized Importance	Rationale/Interpretation
$X(w_speed)$	0	0.00%	Optimization found that this input contributed more noise/variance than a useful signal.
$Y(w_angle)$	199	100.00%	Dominant variable: Identified as the most stable, low-noise (integral) predictor of the vehicle's dynamic regime.
$Z(w_rate)$	0	0.00%	Derivative signal: Optimization eliminated it, likely due to high sensitivity to sensor noise (as confirmed in Section 3.7).

A core hypothesis of this study is that vehicle parameters are regime-dependent; i.e., the same model cannot accurately describe both steady-state and transient behaviors using a single parameter set. To investigate this, the model is calibrated using two physically distinct experimental maneuvers, each representing an operational regime:

- **Constant Radius (CR) Maneuvers:**

These quasi-steady tests emphasize the steady-state cornering behavior of the vehicle. The resulting calibration, denoted as $PARAMS_{CR}$, characterizes the equilibrium handling balance and roll stiffness (defining Pole 0.0).

- **Increasing Steer (IS) Maneuvers:**

These slow, transient tests are used to capture damping behavior and nonlinear onset during steering transitions. The calibrated parameter set from these tests, $PARAMS_{IS}$, defines Pole 1.0.

This regime-targeted calibration process rejects the notion of global optimization and instead anchors the model to two physically interpretable poles in the vehicle's operational space.

The complete computational pipeline, from raw data acquisition through smoothing to the validation loop, is depicted in Figure 1.

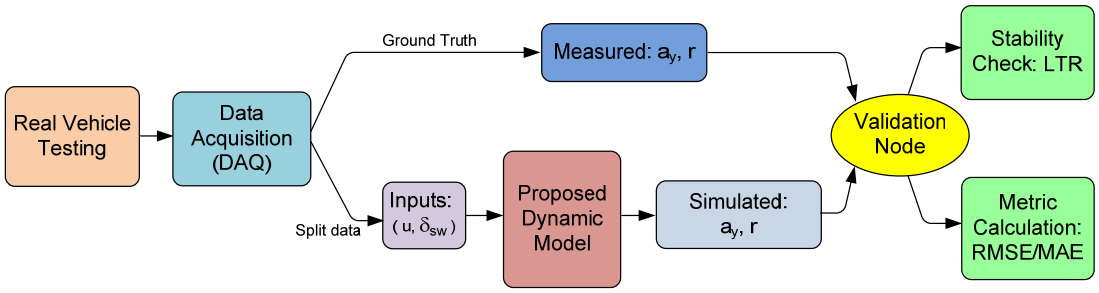


Figure 1. Simulation/validation loop diagram.

2.3. Optimization-Driven Blending Architecture

The overall architecture of the proposed Dynamic Model, illustrating the dual-expert inputs and the blending mechanism, is presented in Figure 2.

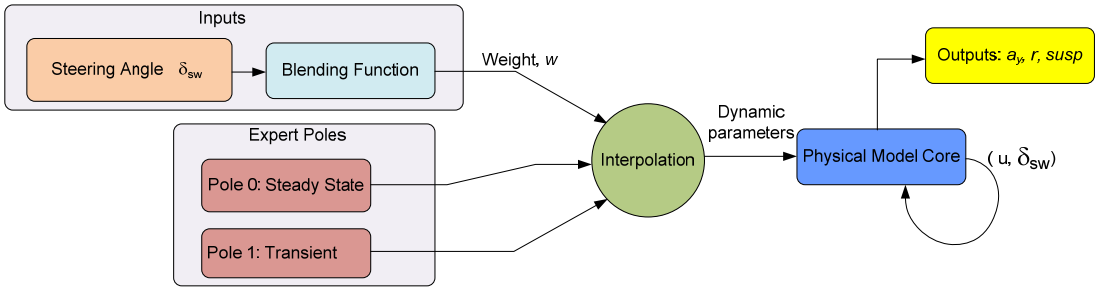


Figure 2. The block diagram of the model architecture.

With the two "expert" parameter sets established, the model requires a mechanism to blend between them dynamically. To determine the most robust scheduling variable, a "meta-optimization" problem is formulated. Three candidate state variables are considered: longitudinal speed (u), steering angle (δ_{sw}), and steering rate ($\dot{\delta}_{\mathrm{sw}}$).

A constrained nonlinear programming solver (fmincon) using the Sequential Quadratic Programming (SQP) algorithm is employed to minimize the error between the calculated blending weight ($\dot{\delta}_{\mathrm{sw}}$) and the ideal target regime ($w_{\mathrm{target.}} = 0$ for steady state; $w_{\mathrm{target}} = 1$ for transient). The cost function is defined as follows:

$$J_{blend} = \sum_{k=1}^{M} \left(w_{blend}(u, \delta, \dot{\delta})_k\right) - \left(w_{\mathrm{target,k}}\right)^2 \tag{7}$$

It is observed that the optimization results converge to a solution where the weights for speed and steering rate are negligible, identifying the steering angle as the dominant and most noise-robust predictor for this class of heavy vehicles. Consequently, the final blending law (Equation (7)) is simplified to an angle-dependent cubic smoothstep function. The transition thresholds are physically anchored: the upper threshold $\delta_{\max}$ is set to 1110 degrees (the vehicle's mechanical steering limit) to ensure full envelope coverage, while the lower threshold $\delta_{\min}$ is set near zero to capture maneuver onset.

The optimization results indicate that the most stable and noise-tolerant configuration is achieved using only the steering wheel angle as the blending variable. The state-dependent blending weight, w_{blend}, is therefore expressed using a smooth cubic transition function between two steering thresholds:

$$w_{blend} = \begin{cases} 0, & \delta_{\mathrm{sw}} \leq \delta_{\min} \\ 3x^2 - 2x^3, & \delta_{\min} < \delta_{sw} < \delta_{\max} \\ 1, & \delta_{sw} \geq \delta_{\max} \end{cases} \tag{8}$$

where $x = \frac{\delta_{sw} - \delta_{\min}}{\delta_{\max} - \delta_{\min}}$, $\delta_{\min} = 0.0001$, $\delta_{\max} = 1110.0$ deg.

Finally, the blended parameter vector is computed as a linear interpolation between the two regime-specific sets:

$$P_{blend} = (1 - w_{blend})P_{CR} + w_{blend}P_{IS} \tag{9}$$

Here, P_{CR} and P_{IS} correspond to the calibrated parameter sets $PARAMS_{CR}$ and $PARAMS_{IS}$ obtained from the CR and IS maneuvers, respectively. This formulation ensures smooth parameter transitions without derivative terms, thereby avoiding the sensitivity issues common to rate-based scheduling strategies. The resulting Dynamic Model thus adapts its effective physical behavior in real time, maintaining both numerical stability and physical plausibility under diverse driving conditions.

3. Results

3.1. Blending Architecture Optimization Results

The first result obtained using the proposed methodology is the systematic selection of the blending variable. The optimization designed to find the optimal weights (X, Y, Z) for the three-input Heuristic Model yielded a conclusive result, as shown in Table 2.

This optimization proved that, for this dataset, the most robust and accurate architecture was the simplest one: the "*Angle-Only*" model. This finding justifies the architecture specified in Section 2.3.

3.2. Dual Calibration Results and Physical Interpretation

The two "expert" parameter sets, calibrated from the CR and IS tests show significant and physically meaningful divergence. These poles (used in Equation 10) define the boundaries of the Dynamic Model's state space.

The clear divergence in Table 3 confirms the hypothesis from Section 1: A single parameter set is insufficient. The vehicle is physically different in these two regimes.

Table 3. Calibrated "expert" parameter sets (poles) for the Dynamic Model.

Parameter	P_{CR} Value	P_{IS} Value	Physical Interpretation
G_{roll}	0.0242	0.0222	Slight decrease in roll gain.
$w_{n,roll}$ (rad/s)	25.0000	12.8257	The quasi-steady-state (CR) regime is much stiffer (higher natural frequency) than the transient (IS) regime.
ζ_{roll}	0.7000	0.9900	Moderate increase in effective damping for the transient regime.
$F_{peak,lat}$ (m/s^2)	6.3720	3.7720	The model associates the steady-state (CR) regime with a higher peak lateral force capability.
$F_{slope,lat}$	2.9009	1.6750	The steady-state (CR) regime is identified as having a much sharper initial tire response (higher slope).

3.3. Generalization and Interpolation Capabilities

To rigorously evaluate the PCH-VDM framework's utility for real-world applications, two distinct generalization tests were conducted using unseen experimental data. These tests challenged the models to predict vehicle behavior outside their calibration envelope (extrapolation) and within intermediate operating points (interpolation). The proposed Dynamic Model (Angle-Only) was compared against a baseline Static Model and a standard Heuristic Model (which uses lateral acceleration, a_y, as the scheduling variable). The quantitative results are summarized in Table 4.

Table 4. Generalization test results on unseen CR25 maneuver (RMSE).

Test Scenario	Metric (RMSE)	Static Model	Dynamic Model	Heuristic Model
Test 1: Extrapolation	a_y (m/s^2)	1.1296	**0.4683**	0.5135
(Training: CR15, IS10, IS15 → Predicting: CR25)	r (rad/s)	0.0951	0.0718	**0.0507**
Test 2: Interpolation	a_y (m/s^2)	0.5663	**0.4687**	0.7402
(Training: CR15, CR25, IS10 → Predicting: IS15)	r (rad/s)	0.2559	**0.1802**	0.2914

In the extrapolation test, the models were trained on lower-dynamic maneuvers (CR15, IS10, and IS15) and tasked with predicting the high-speed constant radius maneuver (CR25). As expected, the Static Model fails to capture the non-linear saturation effects at higher speeds, resulting in a substantial lateral acceleration (a_y,) error of 1.1296 m/s^2. The proposed Dynamic Model demonstrates superior robustness, achieving the lowest a_y, RMSE of 0.4683 m/s^2, effectively halving the error of the static approach. While the Heuristic Model performs adequately in this steady-state scenario, it still lags behind the proposed framework in lateral acceleration accuracy (0.5135 m/s^2), confirming that the angle-based blending strategy provides a more reliable physical description of the vehicle's limit handling.

The interpolation test challenged the models to predict the transient IS15 maneuver after being trained on the surrounding dataset boundaries (CR15, CR25, and IS10). This test proved decisive in exposing the limitations of conventional heuristic approaches. The Heuristic Model exhibits significant performance degradation, yielding the highest errors across all models (RMSE: a_y = 0.7402; r = 0.2914). This failure illustrates the inherent instability of using a response variable (a_y) to schedule model parameters during transient maneuvers, resulting in algebraic loops and poor predictive tracking.

The interpolation test results presented in Table 4 are also clearly visualized in Figure 3. The interpolation test is included here as a representative example of the two generalization tests performed. In the following figures (Figures 3–6), the legend symbols are defined as follows: RD: Real Data (black); SM: Static Model (red); DM:, Dynamic Model (blue); HM: Heuristic Model (green); LL: Lift Limit (dotted black); SL: Static Limit (dotted black).

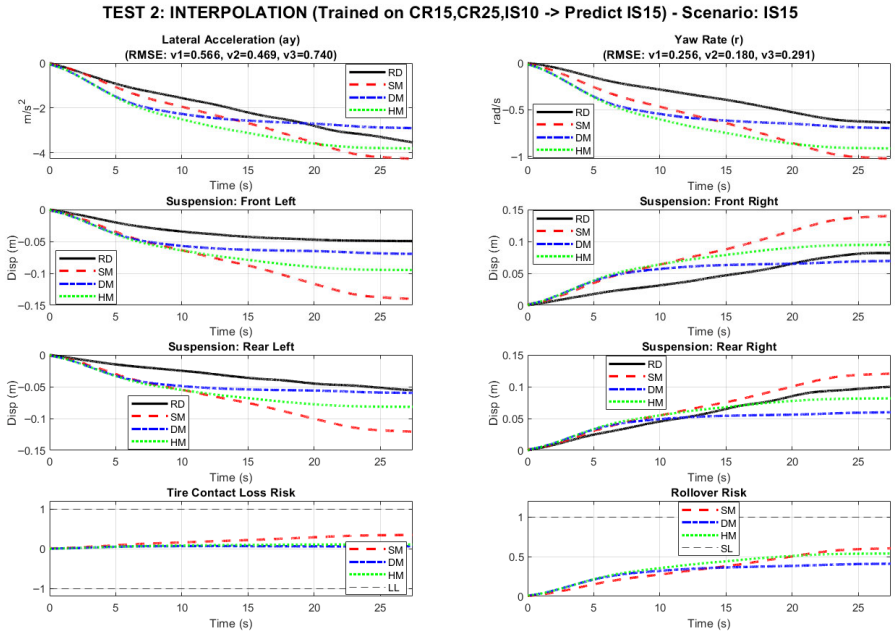


Figure 3. Interpolation test results.

3.4. Performance Across All Dynamic Regimes

Tables 5 and 6 show the average performance across all four real-world test scenarios, comparing the globally optimized Static Model against the Dynamic Model and their ability to match the real test data.

Table 5. Average model performance (per-scenario RMSE).

Scenario	Model	a_y RMSE	r RMSE	Sus_{avg} RMSE
CR15	Static	0.3130	0.0258	0.0130
	Heuristic	0.1459	0.0868	0.0950
	Dynamic	0.1514	0.0824	0.0098
CR25	Static	0.9951	0.0721	0.0196
	Heuristic	0.5135	0.0507	0.0132
	Dynamic	0.4683	0.0718	0.0132
IS10	Static	0.0426	0.0977	0.0068
	Heuristic	0.4776	0.2696	0.0116
	Dynamic	0.1604	0.1141	0.0066
IS15	Static	0.1671	0.1367	0.0182
	Heuristic	0.7402	0.2914	0.0242
	Dynamic	0.4687	0.1802	0.0181

Table 6. Average model performance (overall) and % improvement.

Signal	Static Model Avg. RMSE	Dynamic Model Avg. RMSE	Improvement% (Dynamic vs. Static)	Improvement% (Heuristic vs. Static)
a_y (m/s^2)	0.3794	**0.3122**	17.70%	−23.70%
r (rad/s)	**0.0831**	0.1121	−35.00%	−110.20%
Sus_{avg} (m)	0.0144	**0.0119**	17.30%	−1.40%

The overall average performance and percentage improvement against the Static Model are summarized in Table 5. These results reveal the most critical finding of this study. The "Heuristic" model, which represents a common research approach, fails catastrophically when averaged across all regimes. It degrades a_y accuracy by −23.7% and r accuracy by a significant −110.2% compared to the baseline Static Model.

A detailed look at Table 5 shows the reason for this phenomenon: the Heuristic Model is incapable of handling transient maneuvers (IS10 and IS15), where its a_y RMSE values (0.4776 and 0.7402) are significantly worse than the values of all other models.

In stark contrast, the "Angle-Only" model is the only architecture that provides a net benefit, improving the primary metric a_y by 17.7% and suspension by 17.3%. This demonstrates that the method of blending is not trivial; a poor heuristic choice is significantly worse than doing nothing. The "Angle-Only" method is proven to be the only robust solution, despite its own calculated trade-off (a −35.0% degradation in r).

The model performances numerically presented in Tables 5 and 6 for the CR and IS regimes are also clearly observable in Figure 4 (CR25) and Figure 5 (IS10). Here, the CR25 and IS10 test results are included as representatives of the CR and IS regimes, respectively. While the Heuristic Model (green) produces outputs close to the actual test results in CR25 scenarios, its performance drops dramatically in IS scenarios. It is evident that the Dynamic Model (blue) yields the most balanced and robust results among the models.

Figures 4 and 5 illustrate the comparative performance of the three models during representative CR and ARE tests, respectively. These visual representations corroborate the numerical performance analysis previously conducted via RMSE metrics in the corresponding tables. As clearly evident in both figures, the Dynamic Model (blue) exhibits superior

convergence to the empirical test data (black) compared to both the Heuristic (green) and Static (red) Models.

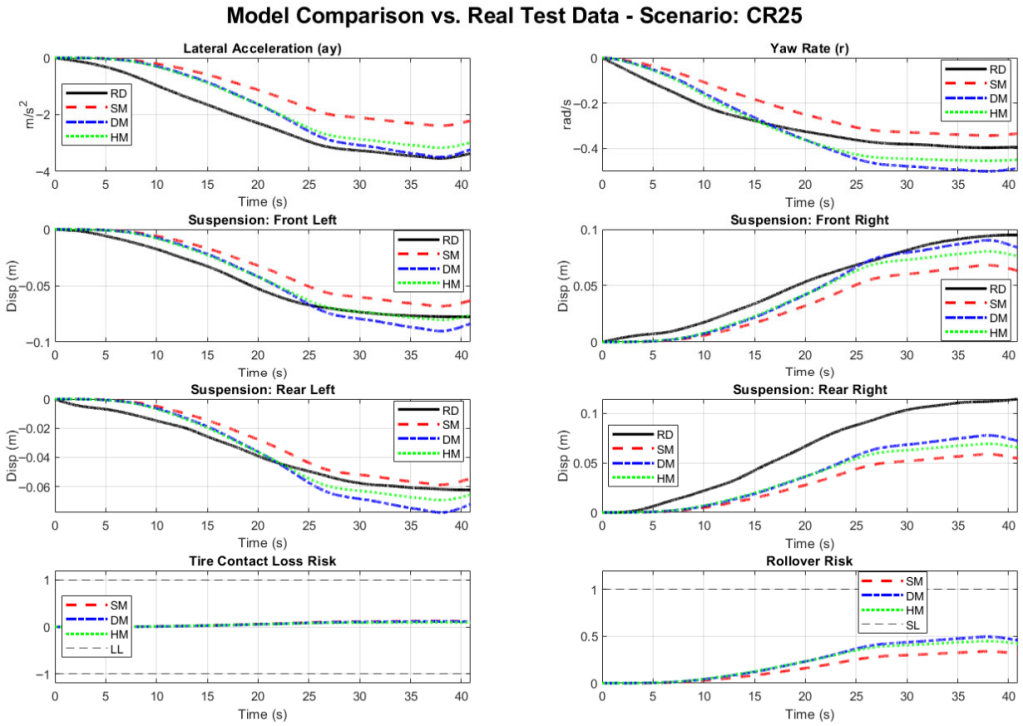


Figure 4. CR25 quasi-steady-state scenario performance.

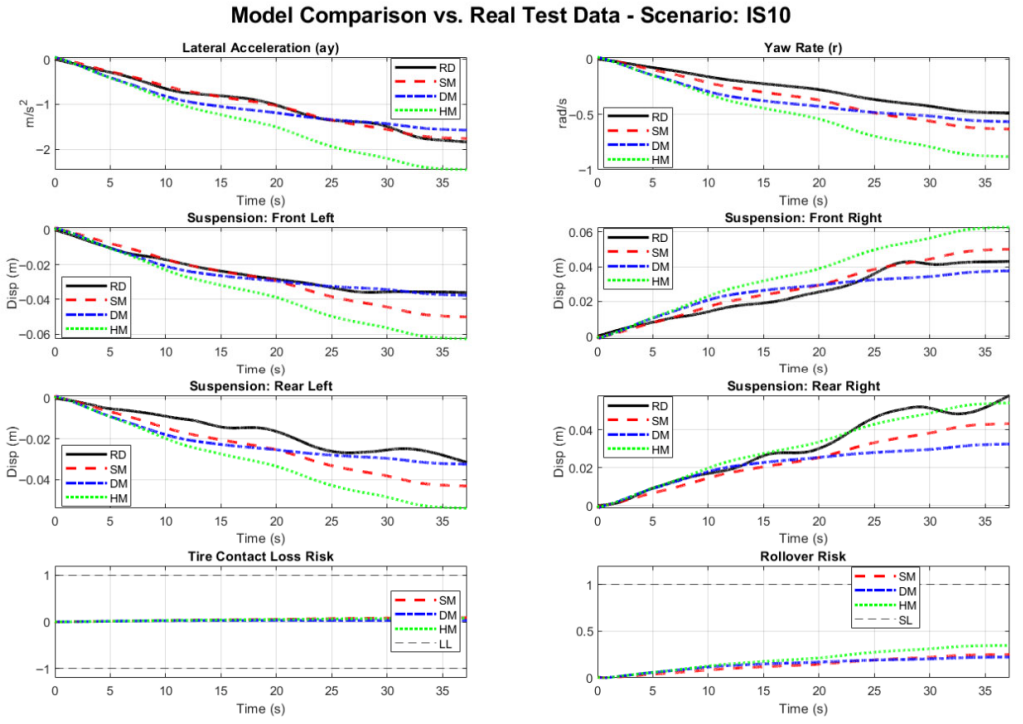


Figure 5. IS10 transient scenario performance.

3.5. Limit-Handling Capabilities in Synthetic Scenarios

A model's true value is its physical plausibility under extreme conditions. The models were tested on aggressive synthetic maneuvers (Double Lane Change and Step Steer, as seen in Table 7).

Table 7. Peak response in synthetic limit-handling scenarios.

Metric	Static Model	Dynamic Model
Double Lane Change Max a_y (m/s^2)	2.5096	3.8785
Double Lane Change Max r (rad/s)	0.1807	0.2793
Step Steer Max a_y (m/s^2)	1.9322	2.9782
Step Steer Max r (rad/s)	0.1391	0.2144

The Static Model produces overly damped, unrealistic responses. The Dynamic Model, by adapting its parameters toward the transient P_{IS} set, correctly predicts significantly higher and more realistic peak responses.

3.6. Model Stability and Physical Plausibility Under Limit Conditions

More critically than the peak values, the behavior of the models diverged. During the aggressive Step Steer test, the Static Model failed catastrophically, exhibiting physically implausible instability and failing to resolve the dynamics.

Figure 6 compares the behavior of the Static Model (red) and Dynamic Model (blue). The Static Model (red) demonstrates a physically implausible and unstable response. The Dynamic Model (blue) remains stable, adaptive, and predictable. The figure provides the most critical evidence. The Static Model's failure is a fundamental breakdown of its physical validity. Its rigid, single-regime parameterization is incapable of representing the required dynamics.

The superior stability of the Dynamic Model, as illustrated in Figure 6, is directly attributable to the physical characteristics of the "Expert Poles" identified during the dual calibration process (Table 3). The Static Model relies on a single parameter set that approximates quasi-steady-state (CR) behavior, which is characterized by a relatively low roll damping ratio ($\zeta_{roll} \approx 0.70$). In contrast, the Dynamic Model adapts to the aggressive step-steer input by shifting its effective parameters toward the transient (IS) pole. As presented in Table 3, the IS pole possesses a significantly higher effective damping ratio ($\zeta_{roll} \approx 0.99$) and a reduced peak lateral force factor ($F_{peak,lat}$ decreases from 6.37 to 3.77). This adaptive shift allows the Dynamic Model to dissipate the sudden energy injection from the step input more effectively, preventing the oscillatory instability and divergence observed in the under-damped Static Model.

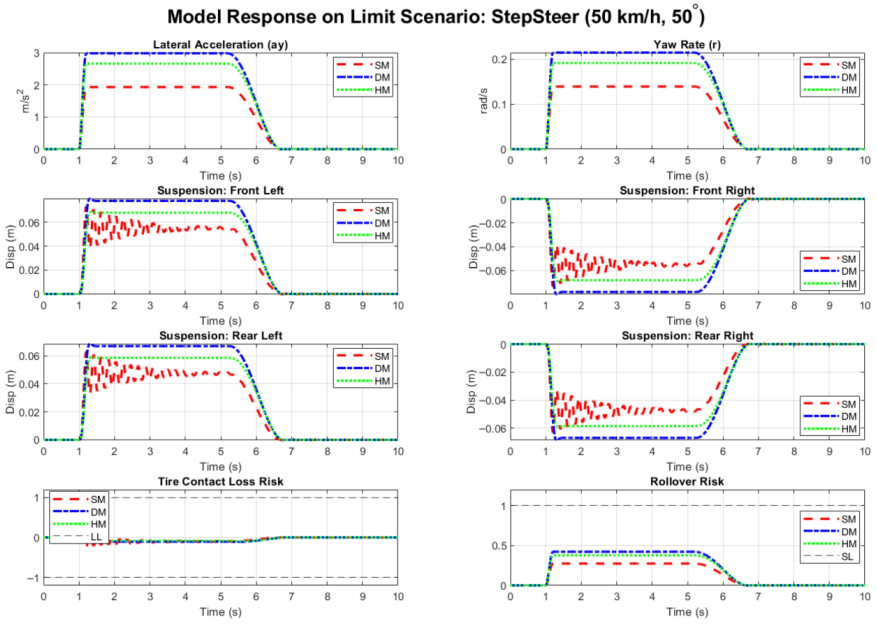


Figure 6. Step Steer stability comparison.

3.7. Robustness to Input Uncertainty: A Monte Carlo Analysis

The robustness of the "Angle-Only" architecture was tested via two Monte Carlo simulations (50 runs each) to simulate sensor noise. Zero-mean Gaussian noise was added to the driver inputs for both a transient (IS15) and a quasi-steady-state (CR25) scenario. The results, measuring the mean standard deviation of the outputs, are shown in Tables 8 and 9.

Table 8. Input noise robustness (base: transient IS15).

Signal	Static Model Std. Dev.	Dynamic Model Std. Dev.
Lateral Acceleration (a_y)	0.0670	0.0764
Yaw Rate (r)	0.0045	0.0059

Table 9. Input noise robustness (base: steady-state CR25).

Signal	Static Model Std. Dev.	Dynamic Model Std. Dev.
Lateral Acceleration (a_y)	0.0370	0.0544
Yaw Rate (r)	0.0042	0.0062

The results confirm the findings from the blending architecture optimization (Table 2). The Dynamic Model, which relies on a blending architecture, exhibits higher variance and is more sensitive to input noise than the simpler foundational model (approximately 14–48% more sensitive depending on the signal and scenario). This is a key component of the bias-variance trade-off and the quantified cost of achieving adaptability.

Robustness against sensor noise and parameter uncertainty is a fundamental requirement for control-oriented models. As quantified in Section 3.7, a Monte Carlo analysis (50 iterations) was conducted by injecting Gaussian noise into the steering and speed inputs. The empirical results (Tables 8 and 9) demonstrate that although the Dynamic Model exhibits a slightly higher output variance than the Static Model, this increase is marginal relative to the performance gains. The observed standard deviations for both yaw rate ($\sigma_r \approx 0.006$ rad/s) and lateral acceleration ($\sigma_{a_y} \approx 0.05 - 0.07$ m/s^2) remain commensurate with the typical signal noise floor observed in heavy-vehicle environments due to engine vibration and sensor quantization. Crucially, this induced variance is an order of magnitude smaller than the accuracy improvements achieved by the model. Furthermore, a supplementary sensitivity analysis (mass/CoG perturbed by $\pm 10\%$) reveals high model resilience; the lateral acceleration RMSE varied by less than 5%. This confirms that the proposed "Angle-Only" blending architecture maintains structural stability without introducing fragility, making it suitable for real-world deployment.

4. Discussion

4.1. Physical Realism and the Justification for Blending

The results demonstrate that the core problem is, in fact, the premise of a single static model. The failure of the Static Model in limit-handling (Figure 6) is a direct consequence of the physical reality exposed in Section 3.2: the quasi-steady-state (CR) test and the transient (IS) test produced two fundamentally different "expert" parameter sets (Table 3).

The P_{CR} set represents a stiff, high-grip model, while the P_{IS} set represents a softer, more compliant model. The Static Model is physically invalid because it is locked into one of these states, causing it to become unstable when the real physics demand a shift. The Dynamic Model succeeds precisely because its architecture is built to acknowledge and bridge this physically proven gap.

4.2. Reframing the a_y/r Trade-Off: A Deliberate Engineering Choice

The central "trade-off" revealed in Table 5—a 17.7% improvement in a_y for a −35.0% degradation in r for the Dynamic Model—must now be re-evaluated in the context of the Heuristic Model benchmark.

This result is interpreted not as a model failure but as a quantified and successful engineering prioritization:

- ➢ *The Primary Goal:* The objective was to fix the Static Model's a_y error and instability. The "Angle-Only" model (Dynamic Model) is the only model that achieves this (17.7% a_y improvement).
- ➢ *The Cost of Failure:* The "Heuristic" model, in its attempt to adapt, failed on all metrics, degrading a_y by −23.7% and r by −110.2%. This demonstrates the high risk of a poorly chosen, non-optimized blending variable.
- ➢ *The Cost of Success:* The −35.0% r -degradation of the proposed Dynamic Model is therefore not only a trade-off but also the minimal, measured cost required to achieve robust adaptation across both steady-state (CR) and transient (IS) regimes. The Heuristic Model proves that a naive approach results in complete failure, validating that the Dynamic Model's performance is the optimal and correct engineering solution.

This is not a "bias–variance trade-off" in the traditional sense of a model flaw but rather a re-prioritization of engineering objectives: moving from a model that is non-plausible in a_y error and unstable to one that is physically plausible and stable at a known cost to a secondary metric (r). The increased noise sensitivity (confirmed in Tables 8 and 9) is also part of this quantified trade-off [33].

4.3. Limitations and Future Research

This methodology—not the model itself—is a prototype. This study has known limitations. The benchmark was confined to the Static Model to highlight the core deficiency of a single parameterization; comprehensive benchmarking against established SOA models (e.g., LPV or FLC) remains a critical step for future validation [13,14,17]. This is a deliberate choice to isolate the methodological contribution (the blending of parameter poles) rather than to compete directly with highly complex SOA models, which, as discussed in Section 1, suffer from their own significant adaptation and re-tuning challenges.

Additionally, the foundational model's one-way coupling (Section 2.1), which omits load-transfer feedback to the lateral force model, was a deliberate decision in the interest of parsimony. This simplification is the likely physical cause of the a_y/r trade-off discussed in Section 4.2. Future research should integrate this physical link, which would likely reduce the r error and noise sensitivity (seen in Tables 8 and 9) simultaneously. Furthermore, this study focuses exclusively on lateral and longitudinal dynamics as the primary objective; integrating Z-axis dynamics (e.g., vertical load transfer feedback) is considered out of the scope of this study but remains a key area for future research.

While the proposed "Angle-Only" blending architecture demonstrated superior robustness for the tested dataset, it is acknowledged that a single scheduling variable may be insufficient for broader operational contexts involving varying payloads or road friction coefficients. Initial optimization attempts with a composite variable (incorporating speed and steering rate) indicated that, for this specific vehicle and maneuver set, additional inputs introduced more noise than a valid signal. However, for future applications, a composite scheduling variable, potentially incorporating a "G-G" diagram index or normalized longitudinal speed, would be necessary to distinguish between high-speed steady-state cornering and low-speed maneuvering.

Furthermore, the current framework relies on a linear interpolation between two distinct regimes (steady state and transient). This methodology is mathematically extensible

to a multi-pole structure to accommodate higher-dimensional operational spaces. The blending equation can be generalized as follows:

$$P_{blend}(x) = \sum_{i=1}^{N} (w_i(x))P_i \tag{10}$$

where P_i represents a vector of "expert parameters" calibrated for specific conditions (e.g., unladen, fully laden, low friction), and $w_i(x)$ represents the weighting function dependent on the vehicle state vector x. Future research will focus on validating this $N - pole$ expansion to capture the effects of load variations and surface friction changes explicitly.

5. Conclusions

This study presents a methodological evolution of a foundational static vehicle model into an adaptive, robust, and physically plausible dynamic model. The core contribution is a pragmatic, two-step methodology for developing such models from sparse data: (1) using regime-targeted calibration (CR vs. IS maneuvers) to define the expert poles and (2) using systematic optimization to prove that a simple "Angle-Only" input is a more robust blending variable than complex, noisy heuristics.

This approach yields a Dynamic Model that solves the Static Model's primary failures: It corrects critical a_y errors and remains physically stable in limit-handling maneuvers where the original model exhibits instability (Figure 6). It is demonstrated quantitatively that this solution is a deliberate engineering reprioritization. The Dynamic Model achieves its primary goals (stability and a_y accuracy) by consciously sacrificing fidelity in a secondary metric—a 35.0% degradation in average r accuracy (Table 6).

It is concluded that this trade-off is not a failure but a success: it is the required cost for achieving physical plausibility and fixing a model's critical flaw. This study serves as a prototype for a methodology that prioritizes real-world applicability and robustness, challenging the pursuit of singular, global optimization in favor of adaptive, multi-objective, and physically grounded solutions. The "usefulness" of a parsimonious model can be dramatically enhanced not by adding complexity but by applying a methodology that allows it to adapt its own core parameters. This study provides a pragmatic path for achieving this balance, demonstrating that even simple models, when methodologically robust, can remain indispensable tools in engineering.

Furthermore, the "Angle-Only" methodology was validated against a "Heuristic" benchmark model. The results prove that the heuristic approach, while intuitive, is highly unstable in transient maneuvers, degrading average a_y performance by over 23% and r performance by over 110% (Table 5). The systematically optimized "Angle-Only" architecture is demonstrated to be the only methodology that successfully improves the primary objective (a_y accuracy) while maintaining physical plausibility across the full operational envelope. This study thus provides a robust new path for model development, proving that the method used to select the blending variable is as critical to success as the concept of blending itself.

Author Contributions: Conceptualization, O.U. and H.Y.; methodology, O.U. and H.Y.; software, O.U. and H.Y.; validation, O.U. and H.Y.; formal analysis, O.U. and H.Y.; investigation, O.U.; resources, O.U.; data curation, H.Y.; writing—original draft preparation, O.U. and H.Y.; writing—review and editing, H.Y.; visualization, O.U.; supervision, H.Y. All authors have read and agreed to the published version of the manuscript.

Funding: This research received no external funding.

Institutional Review Board Statement: Not applicable.

Informed Consent Statement: Not applicable.

Data Availability Statement: The data are not publicly available due to commercial confidentiality/proprietary restrictions.

Conflicts of Interest: Author Ozgur Unsal was employed by the company TEMSA, Adana, Türkiye. The remaining authors declare that the research was conducted in the absence of any commercial or financial relationships that could be construed as a potential conflict of interest.

References

1. Widner, D.; Gnad, T.; Kalcsics, J.; Kőrös, P. Framework for Vehicle Dynamics Model Validation. *Acta Polytech. Hung* **2021**, *18*, 69–88. [CrossRef]
2. Bernard, J.E.; Clover, C.L. *An Investigation into the Validation of Vehicle Dynamics Simulations*; SAE Technical Paper 950308; SAE International: Warrendale, PA, USA, 1995.
3. Salaani, K.; Rao, S.J.; Howe, J.G.; Elsasser, D.; Schnelle, S. *An Applied Review of Simulation Validation Approaches on a Vehicle Dynamics Model*; Report No. DOT HS 813 177; National Highway Traffic Safety Administration: Washington, DC, USA, 2021.
4. Allen, R.; Rosenthal, T.; Szostak, H. *Steady State and Transient Analysis of Ground Vehicle Handling*; SAE Technical Paper 870495; SAE International: Warrendale, PA, USA, 1987.
5. Barthelemy, M. The Role of Parsimonious Models in Addressing Mobility Challenges. *arXiv* **2024**, arXiv:2411.04484. [CrossRef]
6. Della Rossa, F.; Mastinu, G. Analysis of the lateral dynamics of a vehicle and driver model running straight ahead. *Nonlinear Dyn.* **2021**, *104*, 1865–1881. [CrossRef]
7. Holen, P.; Thorvald, B. Possibilities and limitations with distributed damping in heavy vehicles. *Veh. Syst. Dyn.* **2004**, *41*, 172–181.
8. Gong, M.; Chen, H. Variable damping control strategy of a semi-active suspension based on the actuator motion state. *J. Low Freq. Noise Vib. Act. Control* **2019**, *38*, 786–801. [CrossRef]
9. Singh, K.; Sivaramakrishnan, R. *An Adaptive Tire Model for Vehicle Stability Control Systems*; SAE Technical Paper 2015-01-0578; SAE International: Warrendale, PA, USA, 2015.
10. Schiehlen, W. Multibody system dynamics: Roots and perspectives. *Multibody Syst. Dyn.* **1997**, *1*, 149–188. [CrossRef]
11. Galvagno, E.; Galfrè, M.; Mari, G.; Velardocchia, M.; Tota, A. *A Methodology for Parameter Estimation of Nonlinear Single Track Models from Multibody Full Vehicle Simulation*; SAE Technical Paper 2021-01-0336; SAE International: Warrendale, PA, USA, 2021.
12. Ljung, L. *System Identification: Theory for the User*, 2nd ed.; Prentice Hall: Upper Saddle River, NJ, USA, 1999.
13. Leith, D.; Leithead, W. Survey of gain-scheduling analysis and design. *Int. J. Control* **2000**, *73*, 1001–1025. [CrossRef]
14. Li, B.; Rakheja, S. *Yaw Stability Enhancement of Articulated Commercial Vehicles via Gain-Scheduling Optimal Control Approach*; SAE Technical Paper 2017-01-0437; SAE International: Warrendale, PA, USA, 2017.
15. Bokor, Á.; Szabó, Á.; Aradi, S.; Palkovics, L. Design of Gain-Scheduled Lateral Controllers for Autonomous Vehicles. *Eng. Proc.* **2024**, *79*, 38. [CrossRef]
16. Zhang, J.; Sun, W.; Feng, Z. Vehicle yaw stability control via H∞ gain scheduling. *Mech. Syst. Signal Process.* **2018**, *106*, 62–75. [CrossRef]
17. Petrescu, M.; Livint, G.; Lucache, D. Vehicles dynamic control, using fuzzy logic. In Proceedings of the 9th WSEAS International Conference on AUTOMATION and INFORMATION (ICAI'08), Bucharest, Romania, 24–26 June 2008; WSEAS Press: Athens, Greece, 2008; pp. 488–493.
18. Ryu, J. State and Parameter Estimation for Vehicle Dynamics Control Using GPS. Ph.D. Thesis, Stanford University, Stanford, CA, USA, 2004.
19. Cloutier, J.R.; D'Souza, C.N.; Mracek, C.P. Nonlinear Regulation and Nonlinear H-infinity Control via the State-Dependent Riccati Equation Technique. In Proceedings of the First International Conference on Nonlinear Problems in Aviation and Aerospace, Daytona Beach, FL, USA, 9–11 May 1996.
20. Saleem, O.; Filograno, M.L.; Alharbi, S.; Iqbal, J. Hierarchical Fuzzy-Adaptive Position Control of an Active Mass Damper for Enhanced Structural Vibration Suppression. *Mathematics* **2025**, *13*, 2816. [CrossRef]
21. Rasekhipour, Y.; Khajepour, A.; Chen, S. A potential field-based model predictive path-planning controller for autonomous vehicles. *IEEE Trans. Intell. Transp. Syst.* **2017**, *18*, 1295–1307. [CrossRef]
22. Nowakowski, M.; Kosiuczenko, K. Evaluation of TAERO UGV structural collision resistance using FEM analysis. *Bull. Pol. Acad. Sci. Tech. Sci.* **2025**, *73*, e153431. [CrossRef]
23. Dantas, A.E.; Faria, M.T.C. Off-highway truck setup influence on vehicle dynamics and frame durability. *Res. Sq.* 2024; *preprint*. [CrossRef]
24. Vu, V.T.; Sename, O.; Dugard, L.; Gáspár, P. H∞/LPV controller design for an active anti-roll bar system of heavy vehicles using parameter dependent weighting functions. *Heliyon* **2019**, *5*, e01827. [CrossRef]

25. Tjønnås, J.; Johansen, T.A. Stabilization of automotive vehicles using active steering and adaptive brake control allocation. *IEEE Trans. Control Syst. Technol.* **2010**, *18*, 545–558. [CrossRef]
26. Németh, B.; Gáspár, P.; Szabó, Z. Guaranteed performances for a learning-based eco-cruise control using robust LPV method. *IFAC-PapersOnLine* **2021**, *54*, 223–228. [CrossRef]
27. Zatout, M.S.; Rezoug, A.; Rezoug, A.; Baizid, K.; Iqbal, J. Optimisation of fuzzy logic quadrotor attitude controller–particle swarm, cuckoo search and BAT algorithms. *Int. J. Syst. Sci.* **2022**, *53*, 883–908. [CrossRef]
28. Miao, J.; Yan, R.; Zhang, B.; Wen, T.; Li, J.; Fu, Z. Residual Learning Towards High-Fidelity Vehicle Dynamics Modeling With Transformer. *IEEE Robot. Autom. Lett.* **2025**, *10*, 7404–7411. [CrossRef]
29. Chrosniak, J.; Ning, J.; Behl, M. Deep Dynamics: Vehicle Dynamics Modeling with a Physics-Informed Neural Network for Autonomous Racing. *arXiv* **2023**, arXiv:2312.04374. [CrossRef]
30. Hua, L.; Tang, J.; Dourra, H.; Zhu, G. A Gray-Box Surrogate Vehicle Energy Consumption Model Capable of Real-Time Updating. *IEEE/ASME Trans. Mechatron.* **2023**, *28*, 2092–2100. [CrossRef]
31. Lionti, F.; Gutowski, N.; Aubin, S.; Martinet, P. *Bayesian Approach for Parameter Estimation in Vehicle Lateral Dynamics*; Springer: Cham, Switzerland, 2025.
32. Boyali, A.; Thompson, S.; Wong, D.R. Identification of Vehicle Dynamics Parameters Using Simulation-based Inference. *arXiv* **2021**, arXiv:2108.12114. [CrossRef]
33. Friedman, J.; Hastie, T.; Tibshirani, R. *The Elements of Statistical Learning*; Springer: New York, NY, USA, 2001.

Disclaimer/Publisher's Note: The statements, opinions and data contained in all publications are solely those of the individual author(s) and contributor(s) and not of MDPI and/or the editor(s). MDPI and/or the editor(s) disclaim responsibility for any injury to people or property resulting from any ideas, methods, instructions or products referred to in the content.